# AD-A283 797

## REPORT

| | | |
|---|---|---|
| 1 AGENCY USE ONLY | 2 REPORT DATE 1994 | 3 TYPE/DATES COVERED |
| 4 TITLE AND SUBTITLE CORROSION BEHAVIOR OF ALUMINUM-LITHIUM ALLOYS | | 5 FUNDING NUMBERS |
| 6 AUTHOR W N GARRARD | | |
| 7 FORMING ORG NAMES/ADDRESSES DEFENCE SCIENCE AND TECHNOLOGY ORGANIZATION, MATERIALS RESEARCH LABORATORY, PO BOX 50, ASCOT VALE VICTORIA 3032 AUSTRALIA | | 8 PERFORMING ORG. REPORT NO |
| 09 SPONSORING/MONITORING AGENCY NAMES AND ADDRESSES | | |
| 11SUPPLEMENTARY NOTES | | |
| 12 DISTRIBUTION/AVAILABILITY STATEMENT DISTRIBUTION STATEMENT A | | 12B DISTRIBUTION CODE |

13. ABSTRACT (MAX 200 WORDS): CORROSION BEHAVIOR OF THREE ALUMINIUM-LITHIUM ALLOYS WAS INVESTIGATED IN AERATED 0.5m SODIUM SULFATE DEAERATED 3.5% SODIUM CHLORIDE AND AERATED 3.5% NaCl. CORROSION BEHAVIOUR OF THE ALUMINIUM ASSOCIATION ALLOYS 2090-T8E41 (uns a92090) as 8090-T851 (UNS A98090 SHEET) AND AA 8090-T82551 (UNS 98090, BAR) WAS COMPARED TO THE BEHAVIOUR OF THE CONVENTIONAL AA 7075-T6 (UNS A97075SHEET) IN ALL THREE MEDIA, THE SHEET MATERIALS CORRODED AT A SIMILAR RATE, BUT THE BAR FORM OF AA 8090 CORRODED AT A LOWER RATE. PRETREATMENT OF THE ALLOYS BY IMMERSION IN A CERIUM (Ce) SOLUTION INHIBITED PITTING IN AERATED NaCl BUT ONLY FOR A SHORT PERIOD.

| | | | |
|---|---|---|---|
| 14 SUBJECT TERMS | | | 15 NUMBER OF PAGES 9 |
| | | | 16 PRICE CODE |
| 17 SECURITY CLASS.REPORT UNCLASSIFIED | 18 SEC CLASS PAGE UNCLASSIFIED | 19 SEC CLASS ABST. UNCLASS | 20 LIMITATION OF ABSTRACT |



12-PP 94-27240



94 8 25 032

# Corrosion Behavior of Aluminum-Lithium Alloys*

*W.N. Garrard**



## ABSTRACT

*Corrosion behavior of three aluminum-lithium (Al-Li) alloys was investigated in aerated 0.5 M sodium sulfate ($Na_2SO_4$), deaerated 3.5% sodium chloride (NaCl), and aerated 3.5% NaCl. Corrosion behavior of the Aluminum Association (AA) alloys 2090-T8E41 (UNS A92090, sheet), AA 8090-T851 (UNS A98090, sheet), and AA 8090-T82551 (UNS A98090, bar) was compared to behavior of the conventional AA 7075-T6 (UNS A97075, sheet). Uniform corrosion was the predominant form of attack in aerated $Na_2SO_4$ and deaerated NaCl, although some localized attack resulted from corrosion of intermetallics on specimen surfaces. Pitting was the main form of attack in aerated NaCl. In all three media, the sheet materials corroded at a similar rate, but the bar form of AA 8090 corroded at a lower rate. Pretreatment of the alloys by immersion in a cerium (Ce) solution inhibited pitting in aerated NaCl but only for a short period.*

*KEY WORDS: AA 2090, AA 7075, AA 8090, alloying, aluminum, cerium, corrosion, impedance, intergranular attack, lithium, localized corrosion, pitting, polarization resistance, sodium chloride, sodium sulfate*

## INTRODUCTION

New aluminum-lithium (Al-Li) alloys with improved physical characteristics have been developed in recent years for aerospace applications. Each wt% of Li added to an Al alloy increases elastic modulus by 6% and reduces density by 3%.[1] Although Li addition results in an alloy with low ductility and toughness, acceptable mechanical properties can be obtained by using suitable manufacturing processes.[1]

Corrosion behavior of the new alloys has been studied. Sanders and Niskanen summarized early studies of corrosion behavior of Al-Li-X alloys.[2] Generally, increasing the degree of averaging, the number of nucleation sites for δ precipitation, and the amount of Li available to form the δ phase increased corrosion susceptibility. Precipitate-free zones (PFZ) appeared to affect corrosion behavior of the alloys. Moran, et al., suggested Li alone was not a detrimental alloying element with respect to corrosion behavior and that metastable/equilibrium phases containing copper (Cu) or magnesium (Mg) could lead to poor corrosion behavior.[3]

Buchheit, et al.,[4] and Kumai, et al.,[5] have shown Aluminum Association (AA) alloy 2090 (UNS A92090, an Al-Li-Cu alloy with zirconium [Zr])[(1)] underwent pitting and intergranular corrosion (IGC). The primary phases — δ′ ($Al_3Li$), θ′ ($Al_2Cu$), β ($Al_3Zr$), $T_1$ ($Al_2CuLi$), and $T_2$ ($Al_6CuLi_3$) — lead to PFZ along the grain boundaries.[6] Kumai, et al., showed AA 2090-T8E41

* Submitted for publication April 1993; in revised form, August 1993.
* Department of Defence, Defence Science and Technology Organisation, Materials Research Laboratory, P.O. Box 50, Ascot Vale, VIC. 3032, Australia. Present address: Copper Refineries, Ltd., P.O. Box 5484 MC, Townsville, Qld. 4810, Australia.
(1) UNS numbers are listed in *Metals and Alloys in the Unified Numbering System*, published by the Society of Automotive Engineers (SAE) and cosponsored by ASTM.


0010-9312/94/000049/$3.00/0
NACE International

material underwent pitting attack, but that further heat treatment and aging caused intergranular attack (IGA) to occur. IGC was attributed to the copper-free PFZ within the alloy. Buchheit, et al., investigated galvanic coupling between the AA 2090 matrix and the $T_1$ phase and showed the $T_1$ phase was attacked selectively.[4] Buchheit observed two forms of corrosion. The first was the same as observed by Kumai, et al., and resulted in discrete pits on the grain boundaries.[5] Dissolution of the $T_1$ phase was the dominant contribution to this process. In the second type of attack, the initial attack occurred at the periphery of the constituent particles, followed by dissolution of the $T_1$ phase. This mechanism resulted in large pits surrounded by a network of dissolved grain boundaries caused by IGA.

Commercial Al-Li-Mg-Zr alloys (e.g., AA 8090 [UNS A98090]) also contain the δ′, β, and $T_1$ phases along with an S ($Al_2CuMg$) phase. Srivatsan, et al., performed weight-loss measurements on AA 8090 in sodium chloride (NaCl) solutions at various pH levels.[7] As with AA 2090, AA 8090 in solution displayed severe pitting and preferential attack along grain boundaries. The authors suggested microstructural features played a dominant role in the corrosion process. Comparison of the corrosion behavior of AA 8090, AA 7075 (UNS A97075), and AA 2024 (UNS A92024) was performed by Charlton and Hinton.[8] Pitting, associated with constituent particles, and IGA were observed on AA 8090. In contrast to AA 2090, the rate of attack on AA 8090 appeared independent of aging time. The authors concluded AA 8090 was more resistant to corrosion than AA 7075 or AA 2024.

The objective of the present work was to examine the performance of two Al-Li alloys (AA 2090 and AA 8090) and to compare their performance with AA 7075, a material presently in service. Elucidation of the primary mechanism of corrosion was outside the scope of this work.

## EXPERIMENTAL

AA 2090-T8E41 and AA 7075-T6 alloys were rolled sheets 1.6 mm thick. The AA 8090-T851 sheet was 1.44 mm thick, and the AA 8090-T82551 extruded bar was 100 mm by 25 mm in cross section. Elemental compositions are summarized in Table 1.

Sheet specimens (1.5 cm by 1.5 cm) for the electrochemical studies were mounted in epoxy using a hardener so that only one flat face of the sheet was exposed. Electrical contact was made via an insulated wire attached to the back face of the sheet using silver-loaded epoxy. Solution was excluded from the electrical contact by encasing it in epoxy. Samples from the central region of the bar were prepared by machining cylinders (6 mm diam by 15 mm length) such that the cylindrical axis was parallel to the long transverse of the bar or by painting cubic specimens so that each specimen had only one surface, either perpendicular to the rolling direction, long transverse, or short transverse, exposed to the solution. Each specimen was mounted on a specimen holder as described in ASTM Standard G 5-87.[9] No corrosion was observed on the surface hidden under the polytetrafluoroethylene (PTFE) seal of the holder. Cylindrical specimens were used in all experiments unless stated otherwise.

In the electrochemical studies, unpainted samples were polished with various grades of silicon carbide (SiC) paper (up to 1,200 grade), and washed with trichloroethylene, acetone, and distilled water before being introduced into a glass cell (200 $cm^3$) containing the appropriate solution. Painted specimens were polished similarly but were washed only with ethanol and distilled water. Test solutions were aerated 3.5% NaCl and 0.5 M sodium sulfate ($Na_2SO_4$) opened to the atmosphere to allow natural aeration of the solution and deaerated 3.5% NaCl (deoxygenated with high-purity nitrogen [$N_2$], for 1 h before the samples were

**TABLE 1**
*Alloy Chemical Composition*[A]

| Element (%) | Alloy | | | |
|---|---|---|---|---|
| | AA 7075-T6 Sheet | AA 2090-T8E41 Sheet | AA 8090-T851 Sheet | AA 8090-T82551 Bar |
| Si | 0.12 (0.40) | 0.02 (0.1) | 0.02 (0.02) | 0.02 (0.02) |
| Cu | 1.35 (1.20 to 2.00) | 2.60 (2.4 to 3.0) | 1.04 (1.24) | 1.11 (1.23) |
| Mg | 2.82 (2.10 to 2.90) | 0.01 (0.25) | 0.69 (0.67) | 0.65 (0.64) |
| Fe | 0.32 (0.50) | 0.07 (0.12) | 0.04 (0.03) | 0.04 (0.03) |
| Zn | 5.46 (5.10 to 6.10) | 0.01 (0.1) | 0.02 (0.02) | 0.02 (0.02) |
| Ti | 0.04 (0.20) | 0.01 (0.15) | 0.02 (0.02) | 0.02 (0.02) |
| Li | | 1.94 (1.9 to 2.6) | 2.37 (2.35) | 2.37 (2.34) |
| Zr | | 0.14 (0.08 to 0.15) | 0.12 (0.11) | 0.10 (0.1) |
| Cr | 0.18 (0.18 to 0.28) | < 0.01 (0.05) | | |

[A] Expected maximum or range in parentheses.

introduced and covered with a blanket of $N_2$ during the exposure period). Some sheet samples were prepared as above but were immersed in a 1,000 ppm cerous sulfate/0.1 M NaCl solution for 40 days before being transferred to the cell containing aerated 3.5% NaCl. All solutions were prepared using distilled water and analytical-grade reagents.

Separate specimens were used for the various polarization measurements and the alternating current (AC) impedance studies. After each sample was immersed, it was allowed to equilibrate for 3 h before the appropriate response was recorded. Polarization resistance scans were initiated from –30 mV and scanned to +30 mV, with all potentials relative to open-circuit potential (OCP), at a scan rate of 0.2 mV/s. Other polarization scans were performed at a scan rate of 1 mV/s over the range –30 mV to ~ +2,000 mV (relative to OCP). A frequency range of $6.5 \times 10^4$ to 0.01 Hz and a 10 mV AC signal amplitude were used to record AC impedance responses. Impedance measurements were performed at OCP for each specimen. Typically, all polarization curves recorded over the range ± 30 mV of OCP, and the AC impedance spectra were recorded twice daily for 5 days.

Flat or cylindrical platinum (Pt) gauze electrodes were used as counterelectrodes to ensure uniform current distribution over the surface of the similarly shaped specimens. All potentials were referred to a saturated calomel electrode (SCE) or a saturated mercury-mercury sulfate-sodium sulfate ($Hg-Hg_2SO_4-Na_2SO_4$) electrode introduced into the cell via a Luggin probe. A fourth electrode, consisting of a thin Pt wire connected to the reference electrode by a small capacitor (0.5 μF to 1.0 μF), was used in the AC impedance and polarization measurements. This electrode eliminated oscillation problems in the potentiostat control circuitry and eliminated phase shifts during the AC impedance measurements,[10] both of which were attributed to high impedance in the reference electrode/Luggin probe combination. All electrochemical experiments were performed at ambient temperature (22°C ± 3°C).

A potentiostat-galvanostat controlled by a personal computer was used to record all polarization curves. Polarization resistance and instantaneous corrosion rate analyses (PR analyses) were performed using a program written by Hardy and Hanham on data from polarization resistance scans accumulated at a scan rate of 0.2 mV/s.[11] AC impedance spectra were recorded in conjunction with a frequency response analyzer. A purpose-built interface was placed between the current and potential outputs of the potentiostat and the first and second channel inputs of the frequency response analyzer. This arrangement allowed several functions: (1) Auto-zeroing amplifiers could be used to eliminate any direct current (DC) bias in the signals, (2) at frequencies below 1 Hz, optional 40 Hz low-pass filters could be used to filter both channels,[12] and (3) a x1 or x10 gain amplifier could be used in the current channel to increase signal sensitivity. Simulations using various dummy cell configurations showed the interface did not introduce any appreciable errors into the impedance measurements. Detailed information concerning the interface and data collection program have been reported previously.[13] Surface analyses were conducted on specimens used in the AC impedance studies.

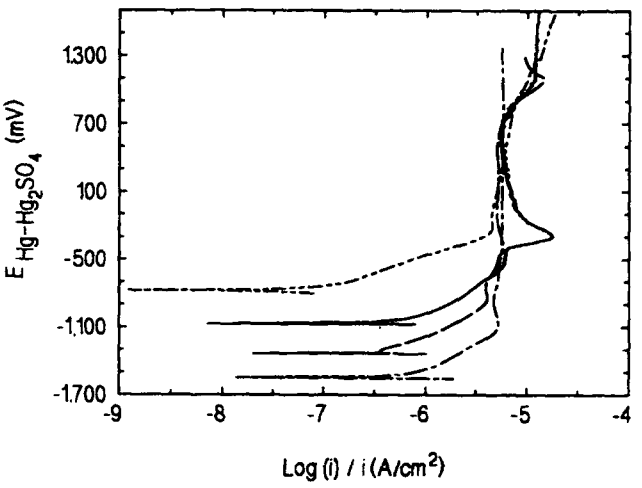


**FIGURE 1.** *Polarization curves for AA 7075-T6 (———), AA 2090-T8E41 (— — —), AA 8090-T851 (— — — —), and AA 8090-T82551 (— — — —) alloys after 3 h immersion in aerated 0.5 M $Na_2SO_4$. Scan rate = 1 mV/s.*

## RESULTS AND DISCUSSION

*DC Polarization Analysis* — Figure 1 displays the polarization curves for the various alloys in aerated 0.5 M $Na_2SO_4$. As anticipated for the non-aggressive medium, all of the alloys displayed passive behavior even at extremely positive potentials. PR analyses of the slow-rate polarization scans for the alloys in aerated 0.5 M $Na_2SO_4$ are summarized in Table 2 (all errors were quoted to 2 standard deviations). Over the 5-day period, AA 7075, AA 2090, and AA 8090-T851 corroded at a similar rate. AA 8090-T82551 material corroded at a lower rate than the other alloys.

All specimens were covered with a very thin layer of oxide after the exposure period. Removal of the oxide revealed relatively shallow pits with diameters ≤ 10 μm in each of the surfaces (Figure 2[a]). Examination of cross sections of the various materials showed these pits were not associated with the grain boundaries within the alloys. The pits most likely arose

**TABLE 2**

*Averaged[A] Corrosion Characteristics for Al Alloys in Aerated 0.5 M $Na_2SO_4$*

| Alloy | $E_{corr}$[B] | $I_{corr}$ ($\mu A/cm^2$) | Corrosion Rate[C] ($\mu m/y$) | $R_p$ ($k\Omega$-$cm^2$) | Pit Depth[D] ($\mu m$) | Local Corr. Rate[E] (mm/y) |
|---|---|---|---|---|---|---|
| AA 7075-T6 Sheet | −925 ± 150 | 0.088 ± 0.02 | 1.0 ± 0.2 | 140 ± 100 | 4.2 ± 0.4 | 0.31 ± 0.03 |
| AA 2090-T8E41 Sheet | −943 ± 100 | 0.12 ± 0.07 | 1.3 ± 0.8 | 110 ± 50 | 3.0 ± 1.0 | 0.22 ± 0.07 |
| AA 8090-T851 Sheet | −1,194 ± 400 | 0.17 ± 0.08 | 1.9 ± 0.9 | 160 ± 80 | 5.5 ± 1.0 | 0.40 ± 0.07 |
| AA 8090-T82551[F] Bar (cylinder) | −795 ± 60 | 0.036 ± 0.01 | 0.39 ± 0.2 | 560 ± 300 | N/D[G] | N/D |

[A] Averaged over a 5-day period and obtained using a scan rate of 0.2 mV/s.
[B] OCP (relative to a saturated $Hg\text{-}Hg_2SO_4\text{-}Na_2SO_4$ electrode).
[C] Derived from $I_{corr}$.
[D] Average depth after exposure period (by optical microscopy).
[E] Derived from pit depth.
[F] Shape of specimen shown in brackets.
[G] N/D = not determined.

from dissolution of intermetallic species present in the alloys. Once the intermetallics dissolved, the underlying Al alloy passivated and protected the material from further corrosion. This passivation after dissolution would explain the shallow depth of the observed pits. Analysis of the pit depths allowed estimation of the local corrosion rate (Table 2). A comparison of the two sets of corrosion rates presented in the table showed similar corrosion rates for all the materials, but a difference of ~ 2 orders of magnitude in the rates in the two sets of data. This difference presumably was the result of the contrasting modes of attack measured by the above procedures. Pit analysis measured the corrosion rate of the intermetallics in the surface of the material. PR analysis, however, resulted in a measure of the rate of uniform corrosion of the surface or a combination of uniform corrosion along with intermetallic dissolution (depending on the relative activity of the intermetallics compared to the Al-Li alloy and the quantity of intermetallics present). After all intermetallics in the surface were removed, PR analysis was expected to provide a more reliable value for the uniform corrosion rate.

Polarization curves (Figure 3) confirmed that, while the materials in deaerated 3.5% NaCl were active at potentials more positive than their respective pitting potentials ($E_{pit}$), the alloys also displayed passive-type behavior. The current in this passive region always was erratic and significantly higher than expected for a true passive state. The potential range of the region varied from one recording to the next. For some alloys, the passive region was absent in repeat experiments. The erratic nature of the current in the passive region suggested a thin oxide protected the various alloys but that the oxide was continually undergoing breakdown and repair during the polarization scan.

$E_{pit}$ were estimated from the polarization curves (Table 3). $E_{pit}$ for the different alloys moved to more positive potentials in the order AA 7075, AA 8090 (both sheet and bar), and AA 2090. Because corrosion potentials ($E_{corr}$) were much more negative than the corresponding $E_{pit}$, no significant pitting was observed on surfaces of the alloys. The small pits observed most likely arose from dissolution of the more active intermetallics present in the surface of each specimen, that is, the same mode of attack as in $Na_2SO_4$ solution. The pits were of similar depth on specimens that had been exposed to the two solutions.

Table 3 summarizes corrosion characteristics of the alloys in deaerated 3.5% NaCl. During the exposure period, PR analysis indicated all the sheet materials corroded at approximately the same rate. However, AA 8090-T82551 corroded at a much slower rate regardless of the shape of the exposed material. As with the alloys in $Na_2SO_4$ and for the same reasons, analysis of the pit depths resulted in higher estimates for corrosion rates for the various alloys compared to results from PR analysis.

Polarization curves for the alloys in aerated 3.5% NaCl were similar to those obtained in deaerated NaCl except that $E_{corr}$ values moved to potentials only slightly less negative than $E_{pit}$. Corrosion characteristics for the various alloys in aerated 3.5% NaCl are summarized in Table 4. The relative ranking of all materials by pit depth and polarization measurements was the same as in the other solutions, but in aerated NaCl, the two types of analyses reflected different modes of attack. Pit analysis provided a measure of the rate of pitting, while PR analysis allowed for estimation of the uniform

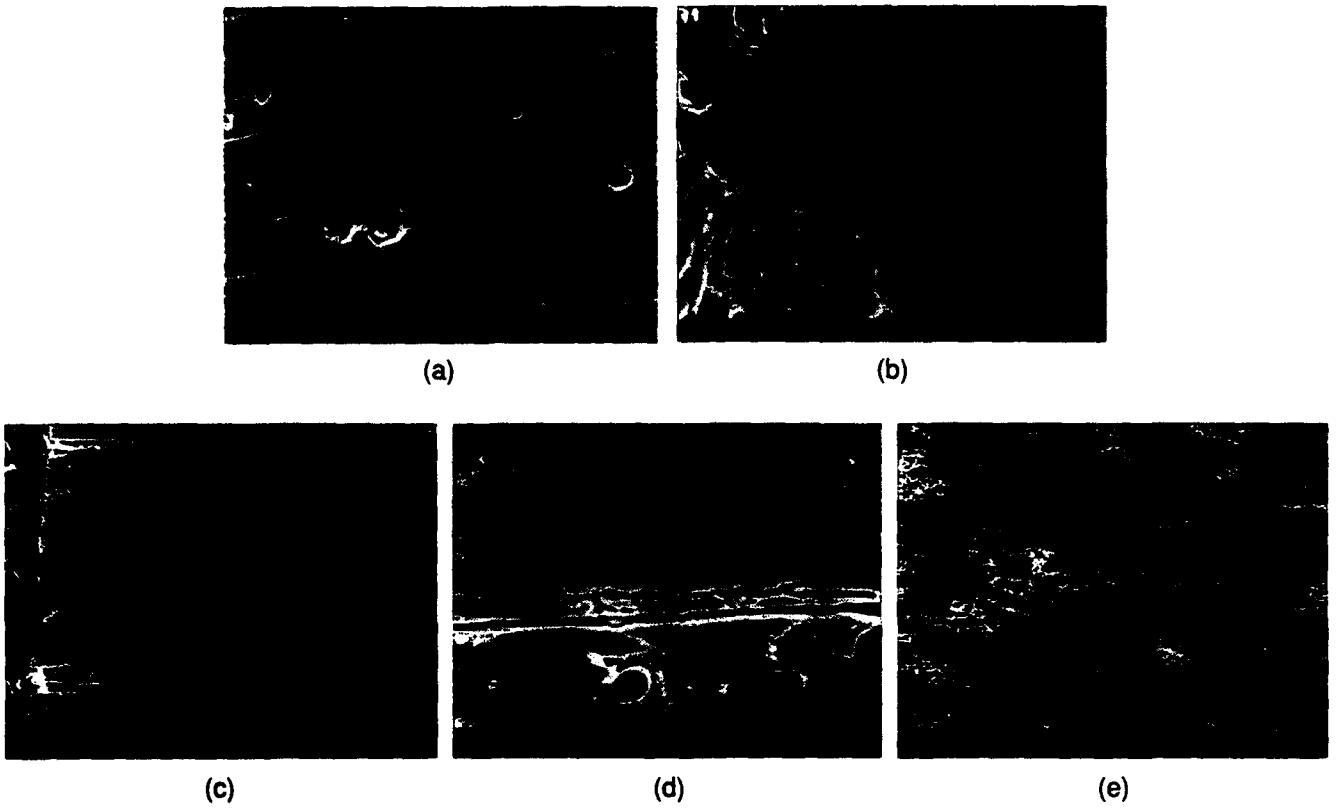


**FIGURE 2.** *Micrographs of various specimens: (a) Surface of AA 2090-T8E41 after 5 days exposure to aerated 0.5 M $Na_2SO_4$ (850x), (b) cross section of AA 8090- T851 after 5 days exposure to aerated 3.5% NaCl (720x), (c) etched (2% sodium hydroxide for 10 min) cross section of AA 8090-T82551 after the surface perpendicular to the rolling direction was exposed to aerated 3.5% NaCl for 5 days (350x), (d) as in (c) except surface perpendicular to the short transverse was exposed to the environment (700x), (e) surface of AA 8090-T82551 perpendicular to the rolling direction after 5 days exposure to aerated 3.5% NaCl (130x).*

corrosion rate, assuming little or no pitting occurred during the slow scan-rate experiments. Observations that the repassivation potential fell between $E_{corr}$ and $E_{pit}$ and that the polarization curves were smooth and showed no increasing current (with time) prior to $E_{pit}$ validated the above assumption.[4] However, the PR analysis results had to be viewed with some caution because the close proximity of $E_{corr}$ and $E_{pit}$ restricted the potential range over which the PR analysis was performed. Relative comparison of the various alloys was impeded further by the different forms of corrosion on the various alloys. AA 7075 underwent severe IGA along its edges, even though the edges were protected by epoxy. The severity of the attack may have been heightened by residual stress introduced when the specimens were guillotined during sample preparation. All the Al-Li materials, however, appeared to corrode by localized attack at the exposed surfaces. It was possible to estimate $E_{pit}$ (after 3 h immersion) for AA 8090-T851 because $E_{corr}$ decreased by ~ 200 mV during the first two days of immersion in aerated 3.5% NaCl. At the end of the exposure period, $E_{corr}$ for this material was similar to its $E_{pit}$.

Since $E_{corr}$ for the various Al-Li alloys were in close proximity to the corresponding $E_{pit}$, alloys in the aerated solution were expected to undergo pitting attack. Optical and electron microscopy of the surfaces of the specimens used in the AC impedance measurements showed large, isolated pits (> 100 μm diam) and a high surface density of small pits (< 100 μm diam) in the sheet-form Al-Li alloys.

Examination of cross sections confirmed growth of the small pits in the alloys was not associated with any microstructural features within the materials. For AA 8090-T851, the bottom of the large pits displayed marked IGA (Figure 2[b]). Slight IGA was observed along with large pits in AA 2090. When the AA 8090 supplied as a bar was examined, pitting was found to be influenced strongly by the presence of grain boundaries (Figures 2[c], [d], and [e]). Modes of the corrosion process in aerated NaCl agreed with those observed by Buchheit, et al.,[4] and Charlton and

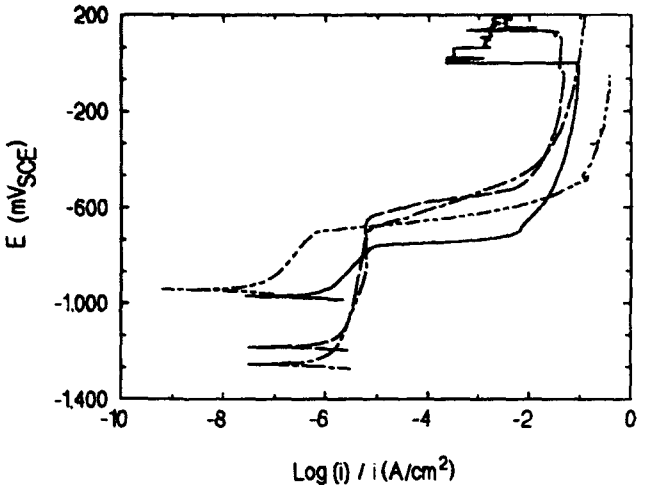


**FIGURE 3.** *Polarization curves for AA 7075-T6 (———), AA 2090-T8E41 (— — —), AA 8090-T851 (— — — —), and AA 8090-T82551 (— — — —) alloys after 3 h immersion in deaerated 3.5% NaCl. Scan rate = 1 mV/s.*

Hinton.[8] Pitting was associated with the constituent particles, and IGA was via dissolution of the $T_1$ phase.

It was possible to compare some of the corrosion characteristics for the various materials with data obtained from other workers, however, Niskanen, et al., showed previously that properties vary with the composition and aging period of Al-Li alloys.[14] For example, $E_{pit}$ in 3.5% NaCl for the alloys in the present work were comparable with results of Charlton and Hinton[8] for AA 8090 (–700 mV) and Kumai, et al.,[5] for AA 2090 (–630 mV). However, the corrosion currents in the present study were ~ 1 order of magnitude lower than currents observed by Charlton and Hinton (the exact temper of their AA 8090 was not specified). In general, characteristic potentials reported in the present work agreed with previous reports, but the corrosion rates differed. The differences possibly reflected the various tempering conditions and environments used by other authors or may have been a reflection of the different methods (e.g., current extrapolation to $E_{corr}$ and weight loss) used to calculate corrosion rates.

In summary, for each solution used, corrosion rates determined from polarization curves indicated all the sheet materials corroded at a similar rate. The extruded bar, however, always corroded at a slower rate than the sheet materials in all three media. This fact may have reflected the different surface structures of the sheet and bar specimens exposed to the solutions. Differing corrosion rates for the bar when various cross sections were exposed to the corrosive medium tended to support this hypothesis. The corrosion rates estimated from the pit depths were much higher than those estimated by PR analysis. In

**TABLE 3**
*Averaged[A] Corrosion Characteristics for Al Alloys in Aerated 3.5% NaCl*

| Alloy | $E_{corr}$[B] | $E_{pit}$[C] (mV) | $I_{corr}$ (μA/cm$^2$) | Corr. Rate[D] (μm/y) | $R_p$ (kΩ-cm$^2$) | Pit Depth[E] (μm) | Local Corr. Rate[F] (mm/y) |
|---|---|---|---|---|---|---|---|
| AA 7075-T6 Sheet | –1,059 ± 122 | –758 | 0.53 ± 0.1 | 5.8 ± 1.0 | 20 ± 9 | 3.8 ± 2.0 | 0.28 ± 0.2 |
| AA 2090-T8E41 Sheet | –1,146 ± 65 | –641 | 0.84 ± 0.7 | 9.2 ± 7.0 | 10 ± 6 | 7.0 ± 2.0 | 0.51 ± 0.2 |
| AA 8090-T851 Sheet | –1,231 ± 19 | –694 | 0.61 ± 0.3 | 6.6 ± 4.0 | 16 ± 10 | 3.3 ± 3.0 | 0.24 ± 0.3 |
| AA 8090-T82551[G] Bar (cylinder) | –930 ± 48 | –704 | 0.0097 ± 0.009 | 0.11 ± 0.1 | 660 ± 300 | N/D[H] | N/D |
| AA 8090-T82551[G] Bar (cube – RD) | –872 ± 122 | N/D | 0.084 ± 0.1 | 0.92 ± 1.0 | 330 ± 700 | 3.4 ± 2.0 | 0.25 ± 0.2 |
| AA 8090-T82551[G] Bar (cube – LT) | –908 ± 150 | N/D | 0.060 ± 0.1 | 0.65 ± 1.0 | 280 ± 400 | 3.2 ± 2.0 | 0.23 ± 0.2 |
| AA 8090-T82551[G] Bar (cube – ST) | –1,004 ± 131 | N/D | 0.017 ± 0.01 | 0.19 ± 0.2 | 600 ± 300 | 4.0 ± 2.0 | 0.29 ± 0.2 |

[A] Averaged over an 8-day (AA 8090-T82551 cubic specimens) or 5-day (other specimens) period and obtained using a scan rate of 0.2 mV/s.
[B] OCP (relative to SCE).
[C] Estimated from polarization scans to ~ +2.0 $V_{SCE}$.
[D] Derived from $I_{corr}$.
[E] Average depth after exposure period (by optical microscopy).
[F] Derived from pit depth.
[G] Shape of specimen shown in parentheses (for cubic sample, the face exposed to the solution is also indicated: RD = face perpendicular to rolling direction, LT = face perpendicular to long transverse, and ST = face perpendicular to short transverse).
[H] N/D = not determined.

the case of the materials in deaerated 3.5% NaCl and 0.5 M $Na_2SO_4$, the pit depth analysis tended to reflect the dissolution of intermetallics in the surface of the specimens. In these media, the influence of intermetallic corrosion was eliminated by cladding the alloys with pure Al sheet, a process often used with other Al alloys. For all of the materials in aerated 3.5% NaCl, the pit depths provided a measure of the rate of pitting.

*AC Impedance Analysis* — The materials also were studied using AC impedance. In aerated 0.5 M $Na_2SO_4$ and deaerated 3.5% NaCl, two methods of analysis of the impedance data seemed appropriate. The first was based on the work of Armstrong and Edmondson, who derived a mathematical expression for the passive film-solution interface from the rates of exchange of both anions and cations from both sides of the interface.[15] Several limiting cases, leading to distinct Nyquist plots, were possible depending on relaxation time of the interface.[16] The alternate method of analysis was based on an equivalent circuit similar to the one proposed by Frers, et al., for Al in chloride medium.[17] Typical Nyquist plots for the alloys in this study are displayed in Figures 4 (aerated 0.5 M $Na_2SO_4$) and 5 (deaerated 3.5% NaCl). Most materials in both solutions displayed one well-defined semicircle at high frequencies and the start of another semicircle at lower frequencies. Armstrong and Edmondson predicted the appearance of two semicircles when the reciprocal of the relaxation time was much less than the applied frequency.[15] While it was possible to extract the rate constants for anion or cation exchange from the parameters derived from the impedance analysis, the analysis was difficult to perform. Thus, the circuit model approach was chosen as the method of analysis.

The circuit model used in the present work is shown in Figure 6(a). $R_s$ was the solution resistance, $R_0$ was the resistance of the passive film, $R_{ct}$ was the polarization resistance for the charge-transfer reaction, C was the overall capacitance of the alloy-film-solution interface, and $C_{ct}$ was the pseudo-capacitance associated with the charge-transfer reaction. A better fit between the model and the experimental data was obtained if the capacitances in the circuit were replaced with constant-phase elements (CPE), which were defined by the equation:[18]

$$Z_{cpe} = Z_0/(j\omega)^{\alpha} \qquad (1)$$

where $Z_0$ (equal to C if $\alpha$ equals 1) and $\alpha$ were constants, $\omega$ was the angular frequency, and $j = \sqrt{-1}$. A Voigt circuit[19] (two parallel-RC combinations in series) could have been used to model the experimental data, but Silverman has shown that both circuits are equivalent, provided $C_{ct}$ is much greater than C (as

**TABLE 4**

*Averaged[A] Corrosion Characteristics for Al Alloys in Deaerated 3.5% NaCl*

| Alloy | $E_{corr}$[B] | $E_{pit}$[C] (mV) | $I_{corr}$ ($\mu A/cm^2$) | Corr. Rate[D] ($\mu m/y$) | $R_p$ ($k\Omega$-$cm^2$) | Pit Depth[E] ($\mu m$) | Local Corr. Rate[F] (mm/y) |
|---|---|---|---|---|---|---|---|
| AA 7075-T6 Sheet | –760 ± 40 | –760 | 0.32 ± 0.4 | 3.5 ± 5.0 | 21 ± 10 | N/D | N/D |
| AA 2090-T8E41 Sheet | –733 ± 6 | –680 | 0.32 ± 0.3 | 3.5 ± 3.0 | 22 ± 10 | 26 ± 20 | 1.9 ± 1.0 |
| AA 8090-T851 Sheet | –752 ± 40 | –706 | 0.38 ± 0.6 | 4.1 ± 6.0 | 50 ± 90 | 29 ± 30 | 2.1 ± 2.0 |
| AA 8090-T82551[G] Bar (cylinder) | –736 ± 40 | –700 | 0.078 ± 0.03 | 0.85 ± 0.4 | 72 ± 30 | N/D[H] | N/D |
| AA 8090-T82551[G] Bar (cube – RD) | –804 ± 100 | N/D | 0.22 ± 0.5 | 2.4 ± 5.0 | 76 ± 100 | 34 ± 20 | 1.5 ± 1.0 |
| AA 8090-T82551[G] Bar (cube – LT) | –741 ± 20 | N/D | 0.14 ± 0.2 | 1.5 ± 2.0 | 100 ± 100 | 23 ± 30 | 1.0 ± 1.0 |
| AA 8090-T82551[G] Bar (cube – ST) | –754 ± 20 | N/D | 0.086 ± 0.1 | 0.94 ± 2.0 | 160 ± 300 | 18 ± 20 | 0.82 ± 0.7 |

[A] Averaged over an 8-day (AA 8090-T82551 cubic specimens) or 5-day (other specimens) period and obtained using a scan rate of 0.2 mV/s.
[B] OCP (relative to SCE).
[C] Estimated from polarization scans to ~ +2.0 $V_{SCE}$.
[D] Derived from $I_{corr}$.
[E] Average depth after exposure period (by optical microscopy).
[F] Derived from pit depth.
[G] Shape of specimen shown in parenthesis (for cubic sample, the face exposed to the solution is also indicated: RD = face perpendicular to rolling direction, LT = face perpendicular to long transverse, and ST = face perpendicular to short transverse).
[H] N/D = not determined.

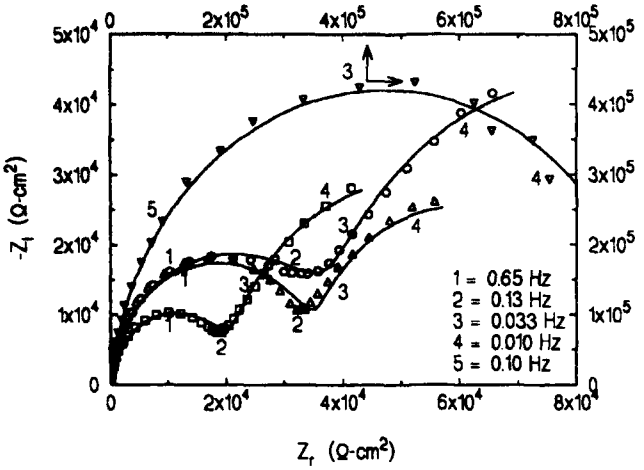


**FIGURE 4.** *Experimental (points) and calculated (lines) impedances for various Al alloys in aerated 0.5 M $Na_2SO_4$: AA 7075-T6, after 1 day of immersion (□); AA 7075-T6, 3 days (○); AA 8090-T851, 2 days (Δ); and AA 8090-T82551, 4 days (▽).*

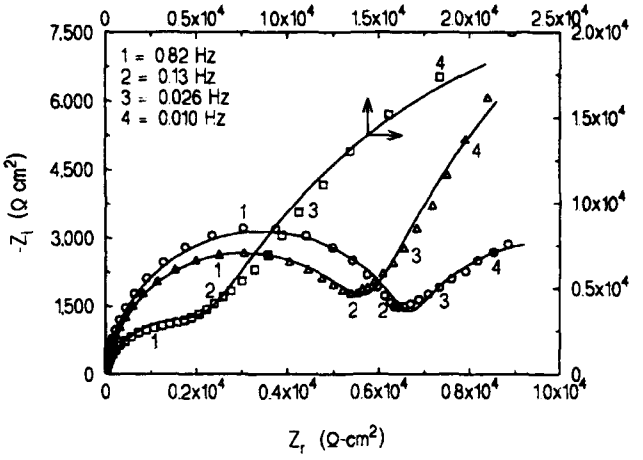


**FIGURE 5.** *Experimental (points) and calculated (lines) impedances for various Al alloys in deaerated 3.5% NaCl: AA 2090-T8E41, after 4 h of immersion (□); AA 2090-T8E41, 5 days (○); and AA 8090-T851, 2 days (Δ).*

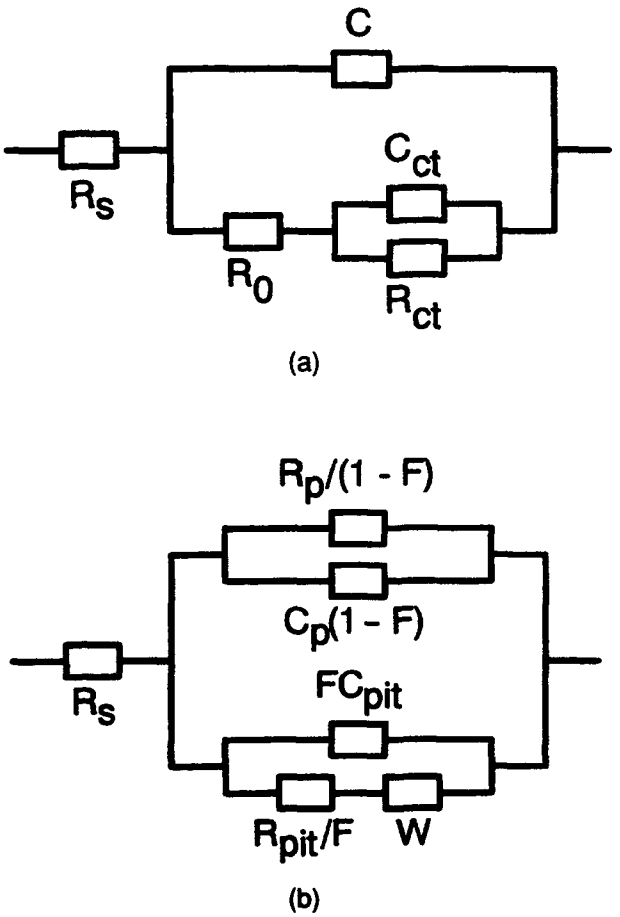


**FIGURE 6.** *Equivalent circuits for the various Al alloys in (a) aerated 0.5 M $Na_2SO_4$ and deaerated 3.5% NaCl and (b) aerated 3.5% NaCl.*

was the case in this work).[20] The average values for the various elements in the circuit model are shown in Table 5. Values were obtained using an analysis software written by Boukamp.[21]

Values for the capacitance (calculated from Equation (1) assuming $\alpha$ equals 1) of the interface were used to estimate the thickness of the oxide layer. The capacitances given in Table 5 were the combination of at least two capacitances, the double-layer capacitance ($C_{dl}$) and the film capacitance ($C_{ox}$), related by the expression:

$$1/C = 1/C_{ox} + 1/C_{dl} \quad (2)$$

Also

$$C_{ox} = \varepsilon\varepsilon_0/\delta \quad (3)$$

where $\varepsilon$ was the dielectric constant (equal to 9 for $Al_2O_3$),[22] $\varepsilon_0$ was the permittivity of free space, and $\delta$ was the thickness of the oxide. While the value of $C_{dl}$ was not available, Equation (3) was used to estimate the upper limit of the oxide thickness for the sulfate and chloride environments (0.6 nm to 1.5 nm and 0.1 nm to 0.8 nm, respectively). The lower thickness for the oxide in 3.5% NaCl was only of the order of one $Al^{3+}$ ion (radius = 0.05 nm) thick. Such a low thickness was not expected and may have been the result of using the geometric area of the electrode instead of the true electrode area (roughness factors of 10 can be envisaged for surfaces polished with 1,200 grade paper). The low thicknesses for the oxides in this study compared to those for Al exposed to a dry (1 nm to

**TABLE 5**
*Averaged[A] AC Impedance Characteristics for Al Alloys in the Indicated Solution*

| Alloy | C[B] (μF/cm²) | $R_0$ (kΩ-cm²) | $C_{ct}$[B] (mF/cm²) | $R_{ct}$ (kΩ-cm²) |
|---|---|---|---|---|
| **Aerated 0.5 M $Na_2SO_4$** | | | | |
| AA 7075-T6 Sheet | 14 ± 6 | 39 ± 60 | 0.23 ± 0.1 | 180 ± 300 |
| AA 2090-T8E41 Sheet | 15 ± 9 | 42 ± 60 | 0.41 ± 0.4 | 110 ± 200 |
| AA 8090-T851 Sheet | 12 ± 6 | 47 ± 50 | 0.35 ± 0.2 | 60 ± 20 |
| AA 8090-T82551[C] Bar (cylinder) | 5.8 ± 2.0 | 780 ± 700 | | |
| **Deaerated 3.5% NaCl** | | | | |
| A 7075-T6 Sheet | 87 ± 50 | 5.2 ± 2.0 | 0.81 ± 0.6 | 24 ± 20 |
| AA 2090-T8E41 Sheet | 38 ± 5 | 6.5 ± 1.0 | 2.0 ± 2.0 | 20 ± 30 |
| AA 8090-T851 Sheet | 40 ± 10 | 6.6 ± 2.0 | 1.9 ± 2.0 | 28 ± 40 |
| AA 8090-T82551[C] Bar (cylinder) | 11 ± 3 | 360 ± 200 | 0.036 ± 0.01 | 810 ± 600 |

[A] Measured at OCP and averaged over a 5-day period.
[B] Capacitance values were obtained from a CPE with a value > 0.79 ($C_{ct}$ in NaCl) or > 0.89 (all other data).
[C] Shape of specimen shown in parentheses.

2 nm) or humid (50 nm to 100 nm) atmosphere suggested a roughness factor between 10 and 100 was appropriate.[23]

Setting the magnitude of C equal to $Z_0$ in Equation (1) regardless of the magnitude of α also influenced the upper estimate for the thickness of the oxide. Numerical analysis of the experimental data using a circuit containing pure capacitors (not CPEs) resulted in values for the capacitances that were 30% to 40% smaller than those tabulated in Table 5, albeit with a significant increase in the "goodness of fit" parameter. Using those capacitance values in the above calculations resulted in higher upper estimates for the film thickness, but a roughness factor much greater than 1 was still required to explain the significant difference between calculated and observed thicknesses.

During the exposure period, C decreased and $R_0$ increased. Such movements were expected as the oxide layer thickened. C and $R_0$ were inversely proportional and proportional to the oxide thickness, respectively. $R_{ct}$, while initially high, tended to decrease for most alloys in the two solutions during the exposure period. $R_{ct}$ values displayed in Table 5 were in fair agreement with $R_p$ values displayed in Tables 2 and 3, which was anticipated. Both referred to the polarization resistance of the electron-transfer reaction. One distinct anomaly in the data was the absence of a second semicircle in the Nyquist plot for the bar-form AA 8090 in aerated $Na_2SO_4$. Either the time-constant ($R_{ct}C_{ct}$) for the semicircle was large and the semicircle only developed at frequencies well below 0.01 Hz, or the time constant was similar to the time constant for the first semicircle, and the two semicircles overlapped significantly. Only extension of the experimental frequency range to lower frequencies (e.g., $10^{-3}$ to $10^{-4}$ Hz) would confirm the first hypothesis. With regard to the second possibility, attempts to fit two overlapping semicircles to the experimental data were successful. However, the final parameters for the two semicircles varied as the initial estimates for the nonlinear least squares were varied. This variation in final parameters may have been affected by noise in the data, which was much higher than in the other data sets.

As shown in Figure 7, Nyquist plots obtained when the alloys were exposed to aerated NaCl were similar in shape to the same plots observed when deaerated NaCl solution was used as the exposure medium. During the first 24 h of exposure, however, some impedance data contained a significant inductive component, probably as a result of adsorption processes at the metal-solution interface. Figure 8 shows the Nyquist plots for the alloys in aerated 3.5% NaCl after treatment with Ce for 40 days before exposure. For the first two to three days, the plots displayed only one semicircle, but after this period, the resultant Nyquist plots displayed two semicircles (similar in nature to the plots obtained for untreated

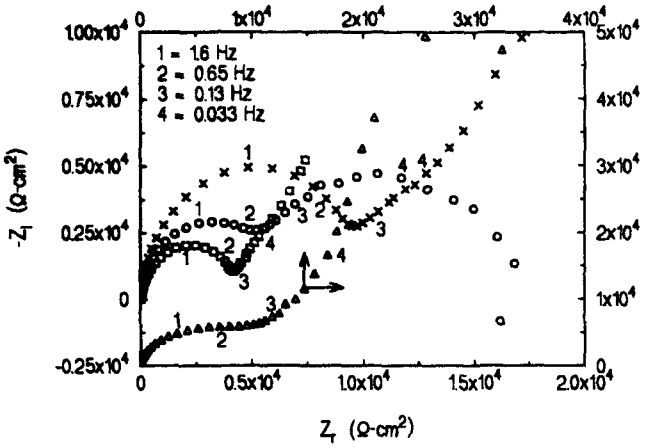


**FIGURE 7.** *Experimental impedances for various Al alloys in aerated 3.5% NaCl: AA 2090-T8E41, after 3 h of immersion (○); AA 2090-T8E41, 3 days (□); AA 8090-T851, 1 day (Δ); and AA 8090-T82551, 4 days (X).*

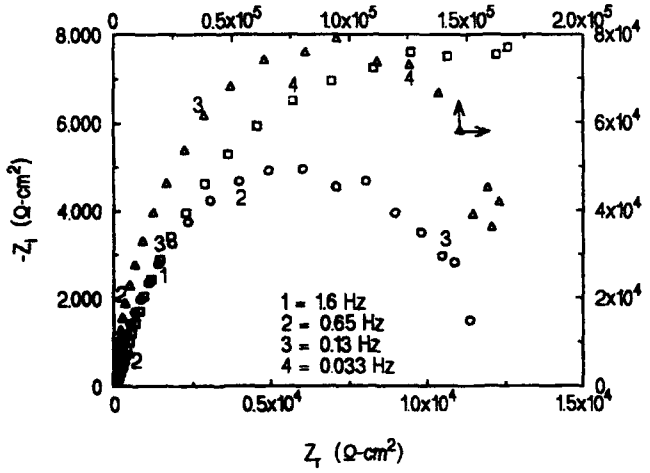


**FIGURE 8.** *Experimental impedances for various Al alloys in aerated 3.5% NaCl after undergoing Ce treatment for 40 days prior to immersion: AA 7075-T6, after 2 days of immersion (○); AA 2090-T8E41, 2 days (□); and AA 8090-T851, 3 days (Δ).*

specimens after 24 h in the same solution). Shih and Mansfeld proposed a circuit description (Figure 6[b]) for materials undergoing active pitting.[24] In their model, $R_{pit}$ was the pitting resistance that indicated the pit growth rate, W described the transmission line behavior of the pits at low frequency, $C_{pit}$ was the capacitance of the pitted area, $R_p$ was the polarization resistance of the passive surface, $C_p$ was the capacitance of the passive surface, $R_s$ was the solution resistance, and F was the area fraction of pitted surface. This circuit was used to analyze the impedance data obtained from the specimens exposed to aerated 3.5% NaCl.

It was not possible to analyze the data according to the procedure of Shih and Mansfeld because the analysis failed at their sixth step.[24] Similarly, attempts to analyze the circuit in Figure 6(b) using the non-linear least squares program written by Boukamp also failed.[21] Analysis of various configurations of the circuit shown in Figure 6(b) using different values for the individual components, however, showed the resistance associated with the high-frequency semicircle prior to pitting, was equivalent to the polarization resistance for uniform corrosion (identical to $R_p$ in Figure 6[b] as F was zero). Once the pitting elements were introduced, analysis of the high-frequency semicircle allowed extraction of the polarization resistance for the pitting process (equivalent to $R_{pit}/F$ in Figure 6[b]). Over the periods of the exposures, values of these two resistances essentially were constant (Table 6). Once pitting occurred on the Ce-treated specimens, the $R_{pit}/F$ values were similar to those obtained for untreated specimens.

Polarization resistance for the Ce-treated AA 7075 prior to pitting was lower than the corresponding data obtained by Shih and Mansfeld for the same material, but the pitting resistance for untreated AA 7075 was similar.[24] The time to pitting (2 days for this work) was significantly shorter than that observed by Shih and Mansfeld (24 days). This time may have been influenced by the presence of residual stress (introduced during guillotining of the specimen), although variation in the treatment conditions may have influenced the pitting time.[25] Thus, initial investigation indicated the Ce pretreatment improved pitting resistance of Al-Li alloys, albeit for only a short period of time. Further work will be required to ascertain the correct pretreatment conditions that would extend the period of increased pitting resistance.

Comparison of resistances obtained by AC impedance measurements with those derived from PR analyses was possible. For all materials in aerated $Na_2SO_4$ and deaerated 3.5% NaCl, there was reasonable agreement between the two data sets ($R_p$ in Tables 2 and 3 and $R_{ct}$ in Table 5) except for AA 8090-T851 in the sulfate medium. In aerated 3.5% NaCl, the resistances calculated from the polarization curves for untreated specimens ($R_p$, Table 4) compared favorably with the same values derived from AC impedance data for Ce-treated specimens ($R_p$, Table 6), but not with the resistances obtained from AC impedance data for untreated materials ($R_{pit}/F$, Table 6). Caution had to be exercised in making this comparison as F was not known. However, microscopic examination indicated it was large for all materials and had only a minor influence on the true

**TABLE 6**
*Averaged[A] Selective AC Impedance Characteristics for Al Alloys in the Aerated 3.5% NaCl*

| Alloy | Ce-Treated Specimens $R_p$[B] (kΩ-cm²) | Untreated Specimens $R_{pit}/F$[C] (kΩ-cm²) |
|---|---|---|
| AA 7075-T6 Sheet | 12 ± 2 | 3.6 ± 0.8 |
| AA 2090-T8E41 Sheet | 22 ± 2 | 5.1 ± 1.0 |
| AA 8090-T851 Sheet | 190 ± 20 | 4.5 ± 0.3 |
| AA 8090-T82551[D] Bar (cylinder) | N/D[E] | 14 ± 4 |

[A] Measured at OCP and averaged over a 2- to 3-day (Ce-treated specimens) or 5-day (untreated specimens) period.
[B] Polarization resistance for uniform corrosion prior to pitting.
[C] Polarization resistance of the pitting reaction during active pitting.
[D] Shape of specimens shown in parentheses.
[E] N/D = not determined.

value of $R_{pit}$. The lower resistances for untreated materials from AC impedance measurements, compared to values obtained from polarization experiments, provided further evidence that results of the PR analyses in aerated 3.5% NaCl were not influenced significantly by pitting.

The laboratory results presented in this work may not have been a true reflection of the behavior of these alloys in service because laboratory conditions could not simulate fluctuations of environmental conditions and the actual environment. For these reasons, exposure trials in marine, tropical, and dry environments are underway to ascertain the corrosion properties of these alloys under service conditions.

## CONCLUSIONS

- In aerated 0.5 M $Na_2SO_4$, deaerated 3.5% NaCl, and aerated 3.5% NaCl the Al-Li alloys AA 2090-T8E41 (sheet) and AA 8090-T851 (sheet) corroded at a similar rate, as estimated by PR analysis, to that of AA 7075-T6 (sheet). The corrosion rate for AA 8090-T82551 (bar) was lower than that for the other alloys. The lower corrosion rate for AA 8090-T82551 was the result of a different surface structure of this alloy compared to the other materials.
- When estimates for the corrosion rates were obtained from an analysis of the pit depths, the ranking of the various materials was the same as that obtained from polarization measurements. Whereas polarization measurements estimated the uniform corrosion rates, pit depth analysis provided a measure of the rate of localized attack. In aerated $Na_2SO_4$ and deaerated NaCl, the localized attack probably resulted from corrosion of intermetallics in the surfaces of the specimens. In aerated NaCl, pitting was the main form of localized corrosion.
- Measurements using AC impedance resulted in the same ranking of the various materials in the three solutions. Initial studies examining the use of Ce pretreatment to enhance the corrosion resistance of the Al-Li alloys showed Ce inhibited pitting attack, albeit for only a short period.

## REFERENCES


1. E.J. Lavernia, N.J. Grant, J. Mater. Sci. 22 (1987): p. 1,521.
2. T.H. Sanders, Jr., P.W. Niskanen, Res. Mechanica Letters 1 (1981): p. 363.
3. J.P. Moran, E.A. Starke, Jr., G.E. Stoner, G.L. Cahen, Jr., Corrosion 43 (1987): p. 374.
4. R.G. Buchheit, Jr., J.P. Moran, G.E. Stoner, Corrosion 46 (1990): p. 610.
5. C. Kumai, J. Kusinski, G. Thomas, T.M. Devine, Corrosion 45 (1989): p. 294.
6. K.T. Venkateswara Rao, R.O. Ritchie, Mater. Sci. Technol. 5 (1989): p. 882.
7. T.S. Srivatsan, T.S. Sudarshan, G.E. Bobeck, Brit. Corros. J. 25 (1990): p. 39.
8. P.J. Charlton, B.R.W. Hinton, "Corrosion of Al-Li-Cu-Mg-Zr Alloy 8090," Proc. Pacific Corrosion, Melbourne, Australia, 1987, Vol. 2, (Melbourne, Australia: Australasian Corrosion Association, 1987), p. 1-7.
9. ASTM Standard G 5-87, Annual Book of ASTM Standards, Vol. 03.02, (Philadelphia, PA: ASTM, 1991), p. 73-79, 1991.
10. F. Mansfeld, S. Lin, Y.C. Chen, H. Shih, J. Electrochem. Soc. 135 (1988): p. 906.
11. A.E. Hardy, C.M. Hanham, "IBM PC Analysis of Polarization Resistance Data," Canadian Defence Technical Communication, 89/307, Defence Research Establishment Atlantic, Dartmouth, July, 1989.
12. M.W. Kendig, A.T. Allen, F. Mansfeld, J. Electrochem. Soc. 131 (1984): p. 935.
13. W.N.C. Garrard, Intelligent Instruments and Computers 9 (1991): p. 177.
14. P. Niskanen, T.H. Sanders, Jr., J.G. Rinker, M. Marek, Corros. Sci. 22, (1982): p. 283.
15. R.D. Armstrong, K. Edmondson, Electrochim. Acta. 18 (1973): p. 937.
16. J.R. Macdonald, Impedance Spectroscopy Emphasizing Solid Materials and Systems (New York, NY: John Wiley & Sons, 1987), p. 8.
17. S.E. Frers, M.M. Stefenel, C. Mayer, T. Chierchie, J. Appl. Electrochem. 20 (1990): p. 996.
18. J.R. Macdonald, Impedance Spectroscopy Emphasizing Solid Materials and Systems (New York, NY: John Wiley & Sons, 1987), p. 90-91.
19. J.R. Macdonald, Impedance Spectroscopy Emphasizing Solid Materials and Systems (New York, NY: John Wiley & Sons, 1987), p. 96.
20. D.C. Silverman, Corrosion 47 (1991): p. 87.
21. B.A. Boukamp, Equivalent Circuit (Enschede, The Netherlands: University of Twente).
22. S. Ikonopisov, L. Andreeva, C. Vodenicharov, Electrochim. Acta 15 (1970): p. 421.
23. Corrosion, L.L. Shreir, ed., 2nd ed., Vol. 1 (London, U.K.: Newnes-Butterworths, 1976), p. 1:27.
24. H. Shih, F. Mansfeld, Corrosion 45 (1989): p. 610.
25. B.R.W. Hinton, D.R. Arnott, N.E. Ryan, Mater. Forum 9 (1986): p. 162.